Journal Pre-proofs

Intensification of plasma-catalytic processes via additive manufacturing. Application to non-oxidative methane coupling to ethylene

Fabio Cameli, Marco Scapinello, Evangelos Delikonstantis, Federico Sascha Franchi, Matteo Ambrosetti, Lidia Castoldi, Gianpiero Groppi, Enrico Tronconi, Georgios D. Stefanidis

PII: S1385-8947(24)00205-5
DOI: https://doi.org/10.1016/j.cej.2024.148720
Reference: CEJ 148720

To appear in: *Chemical Engineering Journal*

Received Date: 16 July 2023
Revised Date: 29 December 2023
Accepted Date: 10 January 2024

Please cite this article as: F. Cameli, M. Scapinello, E. Delikonstantis, F. Sascha Franchi, M. Ambrosetti, L. Castoldi, G. Groppi, E. Tronconi, G.D. Stefanidis, Intensification of plasma-catalytic processes via additive manufacturing. Application to non-oxidative methane coupling to ethylene, *Chemical Engineering Journal* (2024), doi: https://doi.org/10.1016/j.cej.2024.148720

Intensification of plasma-catalytic processes via additive manufacturing. Application to non-oxidative methane coupling to ethylene.

Fabio Cameli[a], Marco Scapinello[a], Evangelos Delikonstantis[b], Federico Sascha Franchi[c], Matteo Ambrosetti[c], Lidia Castoldi[c], Gianpiero Groppi[c], Enrico Tronconi[c] and Georgios D. Stefanidis[a,d,*]

[a] Ghent University, Laboratory for Chemical Technology, Gent, Belgium
[b] AristEng S.à r.l., Luxembourg City, Luxembourg

[c] Politecnico di Milano, Laboratory of Catalysis and Catalytic Processes, Dipartimento di Energia, Milano, Italy

[d] National Technical University of Athens, School of Chemical Engineering, Athens, Greece

*Corresponding author: gstefani@mail.ntua.gr

Keywords

Non-thermal plasma, structured catalyst, additive manufacturing, methane valorization

Abstract

Electrification of chemical processes involving stable molecules can be intensified by additive manufacturing of modular catalytic reactors. We perform single pass conversion of methane (CH_4) into ethylene (C_2H_4) via a nanosecond-pulsed discharge (NPD) plasma coupled with tailor-made 3D-printed catalytic periodic open cell structures (POCS) without external heat or H_2. The plasma discharge effectively activates CH_4 yielding an acetylene-rich (C_2H_2) mixture that is hydrogenated in post-plasma with Pd/Al_2O_3 catalyst deposited on three different copper (Cu) POCS. The POCS assembly, embedded in the ground electrode, enables the plasma discharge, while it promotes the hydrogenation reaction via enhanced heat recovery from the plasma zone. The temperature profile inside the catalytic bed flattens due to the high axial thermal conductivity of the (Cu) POCS. 45% CH_4 conversion is attained in the plasma, with overall 28% C_2H_4 yield resulting from post-plasma hydrogenation. All tested POCS drive C_2H_2 conversion above 93% via enhanced convective and conductive heat transfer with the plasma zone.

1. Introduction

Electrification of the chemical industry is poised to drastically change the outlook of chemical manufacturing in the coming years, when process sustainability will be promoted by efficient energy and heat delivery.[1-3] In this scenario, plasma processing could be one of the main enablers by providing highly energetic electrons that activate stable molecules and heat of reaction from molecular collisions/vibrations, allowing non-conventional chemistries.[4-9] Nonetheless, the radical-based chemistry promoted in plasma processes is generally characterized by low selectivity that hampers the overall process feasibility at larger scales.

The most effective way to enhance the selectivity, and in turn the productivity of plasma processes, is to couple the plasma discharge with a catalytic stage.[10,11] The main approaches of plasma catalysis entail placing the catalyst in direct contact with the discharge (in-plasma catalysis) or employing the catalyst for reactions with the outlet stream of the plasma zone (post-plasma catalysis). The former strategy has been widely employed recently, albeit it is mostly limited to Dielectric Barrier Discharge (DBD) and corona set-ups, whereby energy consumption is often higher than other non-thermal plasma systems, and plasma-catalyst interaction is not fully understood and harnessed. The catalyst particles may affect the distribution of the electric field and the plasma discharge which in turn may structurally modify the catalyst.[12-20]

Contrariwise, post-plasma catalysis is more suitable to warm plasmas, whereby thermal equilibrium between electrons and neutral species is not attained but gas temperature rises sufficiently to drive conventional catalytic reactions.[21-24] This type of discharges have the potential of supplying heat for the catalytic reaction through heat dissipation (Joule heating) in the plasma, however no systematic study has been presented on efficient heat integration to date.

An important process that could greatly benefit from the employment of plasma catalysis is methane (CH_4) valorization, due to the capability of plasma to activate the highly stable molecule while allowing decentralized processing through modular reactors.[25,26] The non-oxidative coupling of CH_4 to high-demand ethylene (C_2H_4)[27] has undergone extensive investigation. The target is to attain low energy demand alongside high selectivity and productivity to make this modular process competitive with state-of-the-art steam cracking of naphtha, which is burdened by extensive carbon emissions.[28-36] Nanosecond pulsed discharge (NPD) plasma reactors have shown the highest energy performance in CH_4 activation owing to the intermittent energy delivery provided by electronic collisions [37-39]. Nevertheless, this plasma configuration promotes formation of acetylene (C_2H_2) as major coupling product (>70% selectivity), thus requiring an additional hydrogenation step to boost C_2H_4 productivity.

Herein, we integrate a highly energy efficient NPD plate-to-plate reactor with a customized 3D-printed electrode element that promotes plasma discharge for CH_4 activation while acting as substrate for the catalytic layer that drives hydrogenation of C_2H_2 to C_2H_4. Additive manufacturing of the electrode body and the periodic open cell structures (POCS) used as catalyst support [40-42] enables intensified thermal and chemical integration between plasma and catalyst zones. We study the performance of a Pd/Al_2O_3 catalyst in the hydrogenation reaction of C_2H_2 to C_2H_4 with varying catalyst loading in a conventionally heated reactor. Then, we integrate the catalytic structured electrode in the plasma reactor and perform the single pass conversion of CH_4 to C_2H_4 without adding external heating or H_2. In these conditions we identify the minimum required catalyst loading to drive the post-plasma reaction and we determine the best performing POCS assembly that promotes C_2H_2 conversion through efficient heat integration.

2. Materials and methods

Additive manufacturing of the stainless steel ground electrode body allows a leaner geometry compared to our previous full cylindrical configuration.[38] Hence, heat dissipated in the plasma discharge can be effectively transferred through the metal element, allowing the new assembly to function without an external heating element in the catalytic zone, as noticeable from Figure 1a-b, where a picture of the experimental setup and a schematic of the reactor assembly are presented. The electrode upper side exposed to the plasma discharge comprises a stainless-steel sintered filter (AmesPore) with a porosity of 5 μm that prevents coke deposition on the catalyst bed. POCS exposure to the plasma discharge is not contemplated in this configuration, as the strong electric field would induce instability in the catalyst layer (e.g., metal sputtering). Besides the filter exposed to the plasma, the electrode body hosts the outlet port, a gas inlet for secondary gases, a temperature measuring point and a cartridge heater (Figure 1b). Different (Cu) POCS have been manufactured by AddToShape

with an EOS 3D printer following geometrical cell profiles produced with an engineering design software (nTopology).

(Cu) POCS enable seamless integration of the catalytic unit in the electrode body and allow optimal heat transfer between the catalytic bed and the electrode body, which is granted by the very high radial and axial thermal conductivity provided by lattice structures, the high gas solid rates between the fluid and the solid structure and thermal contact between the structure and the electrode body. Figure 1c shows the three different catalysts supports that are employed in the catalytic chamber (Figure 1b): a gyroid cell (B) and two different diamond cells (A and C, non-cylindrical and cylindrical geometry, respectively). These geometries are not optimized for flow dynamic conditions; however, the vertical channels (0.6 mm opening) are tilted by 25° to prevent gas channeling in the catalytic bed. The diamond spiral (C) possesses comparable specific surface area (i.e., 4074 m^{-1}) to B and A geometries (i.e., 3840 m^{-1} and 4312 m^{-1}, respectively), but it affords less contact points with the electrode walls (Figure 1c). Detailed cell parameters of each geometry are reported in SI.

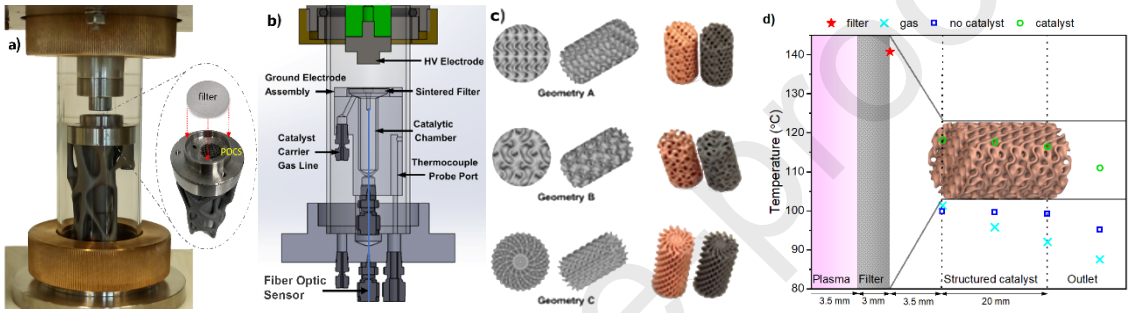

Figure 1. Plasma reactor assembly: (a) photograph of plate-to-plate configuration with 3D printed ground electrode body, (b) sketch of the reactor and (c) 3D printed Cu POCS geometries employed as support for the catalytic layer. (d) Temperature profile in the post-plasma zone with empty catalytic chamber (gas only), and bare and catalytic POCS integrated in the electrode body.

Figure 1d presents a temperature mapping of the post-plasma region obtained via fiber optic (FiSens FBG) measurements (Figure 1b). The temperature profile is obtained under process conditions (CH_4:H_2=1:1 feed) with the fiber optic inserted in the POCS central axis. The external thermocouple port (Figure 1b) allows measuring the electrode body in conditions of external heating, which is outside the scope of this study. The bottom part of the filter exposed to plasma reaches 140 °C as a result of the strong electric discharge hitting the element and the hot gas flowing through. The advantage provided by the highly conductive Cu matrix of the POCS element is highlighted by the temperature profile across the structured element. A temperature drop lower than 1 °C is observed across the (Cu) POCS ('no catalyst' plot in Figure 1d), whereas the temperature of the gas alone plunges by 9 °C along the same distance in the empty catalytic chamber ('gas' plot in Figure 1d). Likewise, the catalytic POCS affords uniform temperature along its longitudinal axis (< 1.7 °C temperature drop), despite operating at higher temperature due to the exothermicity of the catalytic reaction ('catalyst' plot in Figure 1d). The slightly lower temperature at the exit of the POCS is ascribed to the non-adiabatic conditions of the reactor and to the thermal conduction of the metal thermowell of the fiber optic that is partially exposed to the cold ambient atmosphere. These observations suggest that the 3D printed (Cu) POCS enhances heat transfer both via gas-solid interaction with the plasma off gas and heat exchange with the reactor walls in thermal contact with the discharge.

The axial heat redistribution and the enhanced thermal integration allowed by the novel electrode design enables the hydrogenation reaction, contrarily to the previous configuration,[38] where the temperature at the entrance of the bed is not sufficient to trigger the reaction (Figure S3).

The catalyst employed for the post-plasma hydrogenation reaction has been prepared by depositing a catalytic layer (Pd/Al_2O_3) on each 3D-printed (Cu) POCS. The catalyst powder has been prepared via incipient wetness impregnation (SI) and tested for C_2H_2 hydrogenation in a packed bed reactor, tailoring the feed of the system to recreate conditions similar to the plasma experiments. The so-prepared catalytic layer has been deposited on the POCS materials following a 3-step washcoating procedure [43]: dip coating, spin coating, and flash drying; this procedure ensures homogeneous and stable catalyst layers on the Cu supports.

3. Results and discussion

The tests on the Pd/Al_2O_3 catalyst for C_2H_2 hydrogenation (R1) [44] in the conventional packed-bed reactor are reported in Figure 2. Tests are performed at constant gas hourly space velocity (GHSV) referred to the total powder mass. Above 100 °C, C_2H_2 conversion exceeds 98% with all the catalyst loadings employed (i.e., 0.1, 0.5 and 1 wt%). Nevertheless, higher catalyst loading promotes hydrogenation at lower temperature: C_2H_2 conversion at 60 °C is above 40% with 1 wt% Pd/Al_2O_3, whereas it is lower than 25% with 0.5 wt% and no conversion is attained with 0.1 wt%. Due to the reaction exothermicity (R1), increasing C_2H_2 conversion results in a temperature rise that favors kinetics. However, C_2H_4 selectivity starts to decrease at increasing temperature only once C_2H_2 conversion is complete, demonstrating that the reaction is consecutive, and the catalyst is highly selective towards R1. The observed selectivity drop is more pronounced at higher catalyst loading as formation of C_2H_6 is promoted through hydrogenation of C_2H_4 (R2). The negative selectivity in the plot is due to the conversion of the feed C_2H_4.

C_2H_2 hydrogenation to C_2H_4 (R1) benefits from increasing temperature due to enhanced kinetics and catalyst activity. C_2H_4 selectivity strictly depends on the following hydrogenation to C_2H_6 (R2) that is also catalyzed on the Pd surface. Modeling studies have reported a slightly lower activation barrier for C_2H_4 hydrogenation than for C_2H_4 desorption from Pd surface.[45,46] Thereby, temperature increase hinders C_2H_4 and H_2 surface coverage, effectively inhibiting further hydrogenation.

$$C_2H_2 + H_2 \rightarrow C_2H_4 \quad \Delta H_{298K} = -172\frac{kJ}{mol} \qquad (R1)$$

$$C_2H_4 + H_2 \rightarrow C_2H_6 \quad \Delta H_{298K} = -137\frac{kJ}{mol} \qquad (R2)$$

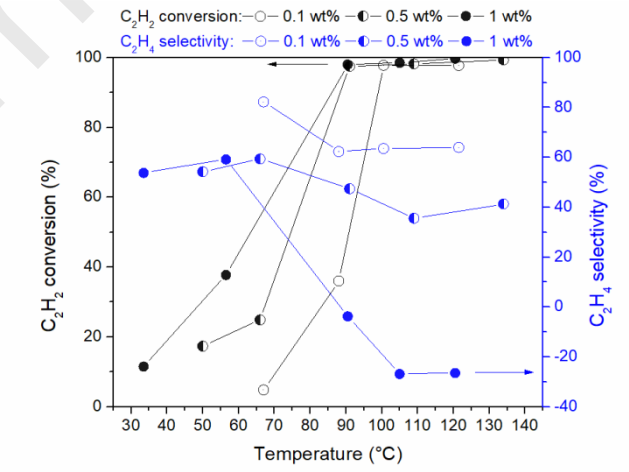

Figure 2. C_2H_2 conversion and C_2H_4 selectivity vs. temperature for different Pd/Al_2O_3 loadings (i.e., 0.1, 0.5, 1 wt%)

The results of Figure 2 confirm these theories as C_2H_4 selectivity increases with temperature until complete C_2H_2 conversion, thereafter C_2H_4 hydrogenation is majorly promoted and undesired C_2H_6 is extensively formed.

The inclusion of 1 wt% Pd/Al_2O_3 catalytic powder in the post-discharge region of the hybrid plasma reactor results in product selectivity similar to that of the fixed-bed experiments (Figure S3): complete hydrogenation of C_2H_2 into C_2H_6 is substantial and hinders C_2H_4 formation. To the contrary, the intensified heat integration granted by the catalytic POCS yields a product selectivity shift in favor of C_2H_4 over C_2H_6.

Figure 3 presents the results of the plasma catalytic experiments conducted with different electrode geometries and catalyst loadings. Constant energy is channelled into the plasma via 3 kHz continuous pulses applied between the electrodes, therefore CH_4 conversion remains constant at 45% throughout the different experiments (Figure S3a). The performance of the reactor is stable over the experimental time of 1 h, which does not allow the onset of extensive carbon deposition to occur. The bare B POCS without catalytic coating features C_2H_2 selectivity of 68% whereas C_2H_4 selectivity is limited to 6%. This set is representative of the gas-phase plasma-assisted CH_4 activation and can be used as benchmark to assess the catalytic activity of the other POCS. Figure 3a presents the effect of Pd catalyst loading on the C_2 species selectivity. Either Al_2O_3 and Cu have no catalytic effect, therefore Pd loading is compared at constant 200 mg Pd/Al_2O_3 on the same Cu POCS geometry (i.e., A cell). The addition of the catalytic layer on the structured electrode enhances C_2H_4 formation even at low Pd loading (i.e., 0.1 wt%) as C_2H_4 selectivity reaches 26%. Comparable C_2H_4 selectivity is observed with 0.5 wt% Pd loading, whilst a shift in C_2 species selectivity is only observed at 1 wt% Pd/Al_2O_3. In this condition C_2H_2 selectivity drops below 1% whilst C_2H_6 formation is promoted via hydrogenation of C_2H_4 that represents the major product with 55% selectivity. Production of heavier hydrocarbon species (e.g., C_3 and C_4) and solid carbon deposition are responsible for the non unitary carbon balance. However, the fixed-bed experiments show that C_4 species are favored over C_3 as the catalyst is ineffective in activating CH_4, whilst the hydrogen balance in the plasma experiments is always around 97%, confirming that solid carbon accounts for the majority of the missing carbon. The heat transfer efficiency is expected to be comparable among different catalyst loadings on the same POCS geometry with constant catalytic layer mass. Nonetheless, more pronounced autothermal effect of the exothermic C_2H_2 hydrogenation reaction at 1 wt% catalyst loading leads to higher bed temperature compared to lower catalytic loadings (Figure 3a). Increasing temperature promoted by the heat of reaction benefits C_2H_4 selectivity as above discussed (Figure 2).

Figure 3b shows that all three POCS geometries employed with 1 wt% Pd loading effectively drive C_2H_2 conversion into C_2H_4 and more limitedly C_2H_6. The gyroid cell B and the diamond cell A attain very similar hydrogenation performances with C_2H_2 conversion above 97%, whereas somewhat lower conversion (i.e., 93%) is obtained with the diamond cell C. Nevertheless, the B POCS features the highest overall C_2H_4 selectivity (i.e., 60 %) and lowest C_2H_6 and C_2H_2 selectivity (i.e., 10% and 2%, respectively), as a result of enhanced heat transfer and increased temperature (Figure 3b) inhibiting C_2H_4 hydrogenation (*R2*, Figure 2).

The total amount of catalyst can be further increased without altering the Pd/Al_2O_3 composition by placing two identical POCS in series or by doubling the amount of Pd/Al_2O_3 catalytic layer on the POCS (Figure 3c). Complete conversion of C_2H_2 is obtained by placing two POCS in series, albeit this condition hampers C_2H_4 selectivity in favor of C_2H_6. These results demonstrate that thermal integration is effective even farther from the plasma discharge, e.g., at double length of the POCS material. Nonetheless, increased contact time promotes C_2H_4 hydrogenation. Similar results are obtained by doubling the catalyst layer amount on the POCS. Thicker catalyst layer does not promote further conversion of C_2H_2 whereas C_2H_4 selectivity slightly drops (from 59 to 57.3%) in favor of C_2H_6 (from 10 to 15.4%) likely due to extended contact time on the catalyst surface.

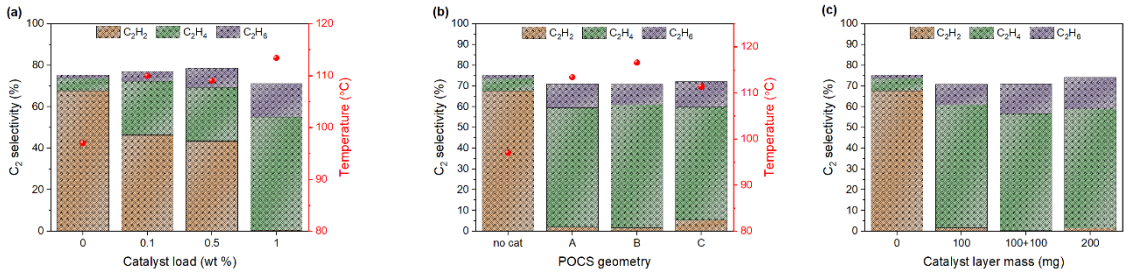

Figure 3. Selectivity of C_2 species (i.e., C_2H_2, C_2H_4 and C_2H_6) at varying (a) loading of Pd catalyst on Al_2O_3 (200 mg) deposited on A POCS (b) POCS geometry with constant catalyst loading (i.e., 1 wt% Pd/Al_2O_3, 100 mg) (c) total mass of Pd/Al_2O_3 catalyst layer (1 wt%) in the catalytic section (i.e., 0, 100 or 200 mg on B POCS or 200 mg total on two B POCS in series).

Decoupling the convective and conductive heat transfer mechanisms is possible by adding an Ar stream before the catalytic POCS (Figure 1b). The gas addition in post discharge does not affect the plasma physics but it decreases both space time and gas temperature. The gas hourly space velocity (GHSV) with Ar addition increases 6-fold compared to the reference condition (i.e., 63107 vs. 10518 h^{-1}). Figure S3a confirms that CH_4 conversion shows negligible variation with varying contact time in the catalytic bed as CH_4 activation is exclusively performed via the plasma discharge upstream. Lower contact time and gas temperature in the catalytic bed hamper C_2H_2 conversion, thereby the product distribution shows an overall lower selectivity of C_2H_4 (Figure S3b) as well as C_2H_6. Post-plasma C_2H_2 conversion across the different POCS with same catalyst loading at high GHSV is an indication of the efficiency of conductive heat transfer, which is the limiting step in these conditions. Figure 4 shows that B and A POCS have similar performances with 61.7 and 55% C_2H_2 conversion, respectively. Contrariwise, C POCS attains only 15% C_2H_2 conversion as a result of poor conductive heat transfer from the electrode wall due to limited contact points between the two surfaces (Figure 1c). The observed conversion trends qualitatively reflect the temperature profiles of the B, A and C POCS that attain 122, 115, and 110 °C, respectively. Similar observations have been made for exothermic processes run in externally cooled reactors loaded with POCS catalyts that were intensified via a metal skin in the outer lateral surface to promote heat transfer.[47] Consequently, C_2H_4 selectivity (based on converted C_2H_2) progressively increases from C to A and B POCS owing to the higher reaction temperature.

In conditions of high gas space velocity and limiting conductive heat transfer, extending the catalytic zone by placing two identical B POCS in series (B+B in Figure 4) is beneficial to C_2H_2 conversion that increases from 61.7 to 85.2% whereas C_2H_4 selectivity drops from 84.7 to 76.8%. Besides catalyst loading on the Al_2O_3 support, the total weight of the catalytic layer deposited on the Cu POCS affects the performance of the process. Increasing the 1 wt% Pd/Al_2O_3 coverage on the B POCS from 100 to 200 mg yields intensified C_2H_2 conversion (i.e., 61.7 to 85.5%, respectively) with a modest C_2H_4 selectivity drop (84.7 to 79.7%, respectively). These results suggest that extending space time by enlarging the catalyst zone enhances C_2H_2 hydrogenation to C_2H_4 at high gas space velocity.

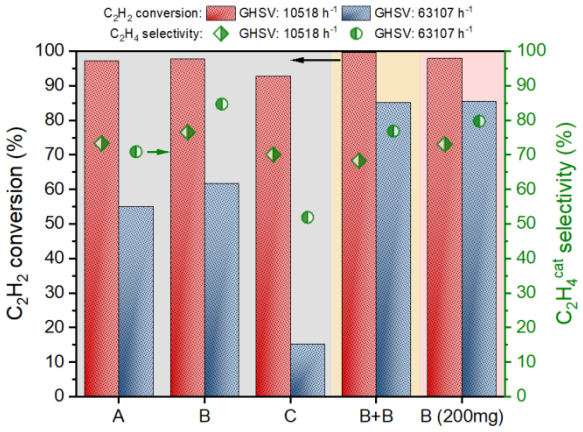

Figure 4. Effect of gas space velocity on C_2H_2 conversion and C_2H_4 selectivity across three different POCS with equal catalyst loading (i.e., 100 mg 1 wt% Pd/Al_2O_3) and across two B POCS (each with 100 mg 1 wt% Pd/Al_2O_3) in series or B POCS with double mass of catalytic layer (i.e., 200 mg 1 wt% Pd/Al_2O_3).

The system proposed herein is not optimized either on the ground of catalyst formulation, or on the energy delivery level. Nonetheless, 25% of the electrical energy is used for CH_4 coupling to C_2H_2, whereas 11% is converted to chemical energy in the overall plasma activation and catalytic hydrogenation. The energy demand of C_2H_4 in the single pass CH_4 coupling is approximately 1700 kJ mol_{C2H4}^{-1}, which is on par with our previous work.[37] However, in that work, a commercial Johnson Matthey catalyst with higher C_2H_4 selectivity from C_2H_2 hydrogenation (i.e., above 90%) had been used, thus compensating for the lower CH_4 conversion in the plasma discharge. In a recent work on gliding arc plasma coupled with a bimetallic Pd-Ag catalyst (which also counterbalances the lower CH_4 conversion) an energy demand of 1340 kJ mol_{C2H4}^{-1} can be calculated, based on data reported by the authors.[23] Nevertheless, an additional N_2 flow is employed in that work to trigger Penning dissociation. For comparison, the implementation of a more selective/commercial hydrogenation catalyst (C_2H_4 selectivity of 90%) in the plasma reactor hereby proposed would require as low as 1150 kJ mol_{C2H4}^{-1}. This would effectively establish this plasma system as a new benchmark for alternative electrified C_2H_4 production routes (e.g., microwave, pulsed compression, and electrically heated reactors), among which plasma-assisted CH_4 coupling already features the highest energy efficiency.[48]

4. Conclusions

In summary, in this study we have integrated a nanosecond pulsed discharge plasma reactor with a structured catalyst to drive non-oxidative CH_4 coupling to C_2H_4 in a single pass without external heat. Three different POCS geometries have been embedded in the ground electrode body that promotes plasma discharge in the plate-to-plate configuration. Besides their role in the electric circuit, POCS support the catalytic layer of Pd/Al_2O_3 that drives hydrogenation of C_2H_2 into C_2H_4 and they efficiently transfer the heat dissipated in the plasma discharge to the catalyst surface. CH_4 activation via the plasma discharge results in 70% C_2H_2 selectivity, whereas the addition of the Pd catalyst in the post-plasma POCS assembly can shift the C_2 species composition up to reaching 60% C_2H_4 selectivity, hence 28% C_2H_4 yield. All three different catalytic POCS can attain C_2H_2 conversion above 93%, nevertheless a gyroid POCS with 1 wt% Pd/Al_2O_3 has shown the most efficient hydrogenation of C_2H_2 due to enhanced heat transfer from the reactor body. Thus, heat integration is key to the hydrogenation reaction as it promotes the activity of the Pd catalyst, and it increases C_2H_4 selectivity as confirmed by

thermocatalytic tests. This reactor configuration can represent a blueprint for future investigations into coupling warm plasmas and a catalytic step running exclusively with plasma-generated heat.

Acknowledgements

This work was performed in the framework of the Moonshot clusterSBO project P2O ("Power-to-olefins: electrified steam cracking and plasma booster"), with the financial support of VLAIO (Flemish Agency for Innovation and Entrepreneurship) via the Flemish spearhead cluster Catalisti.

AddToShape for the realization of the 3D printed POCS materials.

References

1. Schiffer ZJ, Manthiram K: **Electrification and Decarbonization of the Chemical Industry**. *Joule* 2017, **1**:10-14.

2. Barton JL: **Electrification of the chemical industry**. *Science* 2020, **368**:1181-1182.

3. Wismann ST, Engbæk JS, Vendelbo SB, Bendixen FB, Eriksen WL, Aasberg-Petersen K, Frandsen C, Chorkendorff I, Mortensen PM: **Electrified methane reforming: A compact approach to greener industrial hydrogen production**. *Science* 2019, **364**:756-759.

4. Brandenburg R, Bogaerts A, Bongers W, Fridman A, Fridman G, Locke BR, Miller V, Reuter S, Schiorlin M, Verreycken T, Ostrikov K: **White paper on the future of plasma science in environment, for gas conversion and agriculture**. *Plasma Processes and Polymers* 2018, **16**.

5. Weltmann KD, Kolb JF, Holub M, Uhrlandt D, Šimek M, Ostrikov K, Hamaguchi S, Cvelbar U, Černák M, Locke B, et al.: **The future for plasma science and technology**. *Plasma Processes and Polymers* 2018, **16**.

6. Bogaerts A, Neyts EC: **Plasma Technology: An Emerging Technology for Energy Storage**. *ACS Energy Letters* 2018, **3**:1013-1027.

7. Montesano C, Salden TPW, Martini LM, Dilecce G, Tosi P: **CO2 Reduction by Nanosecond-Plasma Discharges: Revealing the Dissociation's Time Scale and the Importance of Pulse Sequence**. *The Journal of Physical Chemistry C* 2023, **127**:10045-10050.

8. Soldatov S, Carbone E, Kuhn A, Link G, Jelonnek J, Dittmeyer R, Navarrete A: **Efficiency of a compact CO2 coaxial plasma torch driven by ultrafast microwave power pulsing: Stability and plasma gas flow dynamics**. *Journal of CO2 Utilization* 2022, **58**:101916.

9. Scapinello M, Delikonstantis E, Stefanidis GD: **The panorama of plasma-assisted non-oxidative methane reforming**. *Chemical Engineering and Processing: Process Intensification* 2017, **117**:120-140.

10. Mehta P, Barboun P, Go DB, Hicks JC, Schneider WF: **Catalysis Enabled by Plasma Activation of Strong Chemical Bonds: A Review**. *ACS Energy Letters* 2019, **4**:1115-1133.

11. Whitehead JC: **Plasma-catalysis: Is it just a question of scale?** *Frontiers of Chemical Science and Engineering* 2019, **13**:264-273.

12. Ma Y, Wang Y, Harding J, Tu X: **Plasma-enhanced N2 fixation in a dielectric barrier discharge reactor: effect of packing materials**. *Plasma Sources Science and Technology* 2021, **30**:105002.

13. Gadkari S, Gu S: **Influence of catalyst packing configuration on the discharge characteristics of dielectric barrier discharge reactors: A numerical investigation**. *Physics of Plasmas* 2018, **25**.

14. Jo S, Kim T, Lee DH, Kang WS, Song Y-H: **Effect of the Electric Conductivity of a Catalyst on Methane Activation in a Dielectric Barrier Discharge Reactor**. *Plasma Chemistry and Plasma Processing* 2013, **34**:175-186.

15. van 't Veer K, van Alphen S, Remy A, Gorbanev Y, De Geyter N, Snyders R, Reniers F, Bogaerts A: **Spatially and temporally non-uniform plasmas: microdischarges from the perspective of molecules in a packed bed plasma reactor**. *Journal of Physics D: Applied Physics* 2021, **54**.

16. Wang W, Butterworth T, Bogaerts A: **Plasma propagation in a single bead DBD reactor at different dielectric constants: insights from fluid modelling**. *Journal of Physics D: Applied Physics* 2021, **54**.

17. Wang W, Kim H-H, Van Laer K, Bogaerts A: **Streamer propagation in a packed bed plasma reactor for plasma catalysis applications**. *Chemical Engineering Journal* 2018, **334**:2467-2479.

18. Engeling KW, Kruszelnicki J, Kushner MJ, Foster JE: **Time-resolved evolution of micro-discharges, surface ionization waves and plasma propagation in a two-dimensional packed bed reactor**. *Plasma Sources Science and Technology* 2018, **27**.

19. Kruszelnicki J, Engeling KW, Foster JE, Kushner MJ: **Interactions between atmospheric pressure plasmas and metallic catalyst particles in packed bed reactors**. *Journal of Physics D: Applied Physics* 2020, **54**.

20. Delikonstantis E, Scapinello M, Sklari SD, Stefanidis GD: **Intensification of a hydrogenation catalyst activity by nanosecond pulsed discharge treatment**. *Plasma Processes and Polymers* 2018, **15**.

21. Zhang H, Li L, Xu R, Huang J, Wang N, Li X, Tu X: **Plasma-enhanced catalytic activation of CO2 in a modified gliding arc reactor**. *Waste Disposal & Sustainable Energy* 2020, **2**:139-150.

22. Chun S, Shin D, Ma S, Yang G, Hong Y: **CO2 Microwave Plasma—Catalytic Reactor for Efficient Reforming of Methane to Syngas**. *Catalysts* 2019, **9**.

23. Zhou M, Yang Z, Ren J, Zhang T, Xu W, Zhang J: **Non-oxidative coupling reaction of methane to hydrogen and ethene via plasma-catalysis process**. *International Journal of Hydrogen Energy* 2022.

24. Girard-Sahun F, Biondo O, Trenchev G, van Rooij G, Bogaerts A: **Carbon bed post-plasma to enhance the CO2 conversion and remove O2 from the product stream**. *Chemical Engineering Journal* 2022, **442**:136268.

25. Gao Y, Neal L, Ding D, Wu W, Baroi C, Gaffney AM, Li F: **Recent Advances in Intensified Ethylene Production—A Review**. *ACS Catalysis* 2019, **9**:8592-8621.

26. Woodall CM, Fan Z, Lou Y, Bhardwaj A, Khatri A, Agrawal M, McCormick CF, Friedmann SJ: **Technology options and policy design to facilitate decarbonization of chemical manufacturing**. *Joule* 2022, **6**:2474-2499.

27. Delikonstantis E, Papaioannou I, Van Geem KM, Stefanidis GD: **Mobile electrified plants for decentralized wasted gas valorization: A solution to face the challenges of the new energy era**. *Energy Conversion and Management* 2023, **285**:117008.

28. Kado S, Sekine Y, Urasaki K, Okazaki K, Nozaki T: **High performance methane conversion into valuable products with spark discharge at room temperature**. In *Studies in Surface Science and Catalysis*. Edited by Bao X, Xu Y: Elsevier; 2004:577-582. vol 147.]

29. Wang K, Li X, Zhu A: **A Green Process for High-Concentration Ethylene and Hydrogen Production from Methane in a Plasma-Followed-by-Catalyst Reactor**. *Plasma Science and Technology* 2011, **13**:77.

30. Liu L, Das S, Zhang Z, Kawi S: **Nonoxidative Coupling of Methane over Ceria-Supported Single-Atom Pt Catalysts in DBD Plasma**. *ACS Applied Materials & Interfaces* 2022, **14**:5363-5375.

31. Wang B, Guan HM: **Highly Efficient Conversion of Methane to Olefins via a Recycle-Plasma-Catalyst Reactor**. *Catalysis Letters* 2016, **146**:2193-2199.

32. Wang K, Li X, Wang H, Shi C, Xu Y, Zhu A: **Oxygen-Free Conversion of Methane to Ethylene in a Plasma-Followed-by-Catalyst (PFC) Reactor**. *Plasma Science and Technology* 2008, **10**:600.

33. Yao S, Nakayama A, Suzuki E: **Methane conversion using a high-frequency pulsed plasma: Discharge features**. *AIChE Journal* 2001, **47**:419-426.

34. Młotek M, Sentek J, Krawczyk K, Schmidt-Szałowski K: **The hybrid plasma–catalytic process for non-oxidative methane coupling to ethylene and ethane**. *Applied Catalysis A: General* 2009, **366**:232-241.

35. Ayodele OB: **Resolving one of the holy grails of catalysis: Direct nonoxidative methane conversion to ethylene over plasma-assisted atomically dispersed Pt catalyst**. *International Journal of Hydrogen Energy* 2022.

36. Maitre P-A, Long J, Bieniek MS, Bannerman MN, Kechagiopoulos PN: **Investigating the effects of helium, argon and hydrogen co-feeding on the non-oxidative coupling of methane in a dielectric barrier discharge reactor**. *Chemical Engineering Science* 2022, **259**:117731.

37. Delikonstantis E, Scapinello M, Stefanidis GD: **Low energy cost conversion of methane to ethylene in a hybrid plasma-catalytic reactor system**. *Fuel Processing Technology* 2018, **176**:33-42.

38. Delikonstantis E, Scapinello M, Van Geenhoven O, Stefanidis GD: **Nanosecond pulsed discharge-driven non-oxidative methane coupling in a plate-to-plate electrode configuration plasma reactor**. *Chemical Engineering Journal* 2020, **380**:122477-122477.

39. Gao Y, Dou L, Feng B, Zhang C, Shao T: **Catalyst-free activation of CH4 and air into platform chemicals and H2 using parametrized nanosecond pulsed plasma**. *Energy Conversion and Management* 2023, **276**:116570.

40. Kapteijn F, Moulijn JA: **Structured catalysts and reactors – Perspectives for demanding applications**. *Catalysis Today* 2022, **383**:5-14.

41. Lämmermann M, Horak G, Schwieger W, Freund H: **Periodic open cellular structures (POCS) for intensification of multiphase reactors: Liquid holdup and two-phase pressure drop**. *Chemical Engineering and Processing - Process Intensification* 2018, **126**:178-189.

42. Tronconi E, Groppi G, Visconti CG: **Structured catalysts for non-adiabatic applications**. *Current Opinion in Chemical Engineering* 2014, **5**:55-67.

43. Balzarotti R, Beretta A, Groppi G, Tronconi E: **A comparison between washcoated and packed copper foams for the intensification of methane steam reforming**. *Reaction Chemistry & Engineering* 2019, **4**:1387-1392.

44. Bos ANR, Westerterp KR: **Mechanism and kinetics of the selective hydrogenation of ethyne and ethene**. *Chemical Engineering and Processing: Process Intensification* 1993, **32**:1-7.

45. Mei D, Neurock M, Smith CM: **Hydrogenation of acetylene–ethylene mixtures over Pd and Pd–Ag alloys: First-principles-based kinetic Monte Carlo simulations**. *Journal of Catalysis* 2009, **268**:181-195.

46. Studt F, Abild-Pedersen F, Bligaard T, Sørensen RZ, Christensen CH, Nørskov JK: **Identification of non-precious metal alloy catalysts for selective hydrogenation of acetylene**. *Science* 2008, **320**:1320-1322.

47. Fratalocchi L, Groppi G, Visconti CG, Lietti L, Tronconi E: **Packed-POCS with skin: A novel concept for the intensification of non-adiabatic catalytic processes demonstrated in the case of the Fischer-Tropsch synthesis**. *Catalysis Today* 2022, **383**:15-20.

48. Delikonstantis E, Cameli F, Stefanidis GD: **Electrified chemical reactors for methane-to-ethylene conversion**. *Current Opinion in Chemical Engineering* 2023, **41**:100927.

Declaration of interests

☒ The authors declare that they have no known competing financial interests or personal relationships that could have appeared to influence the work reported in this paper.

☐ The authors declare the following financial interests/personal relationships which may be considered as potential competing interests:

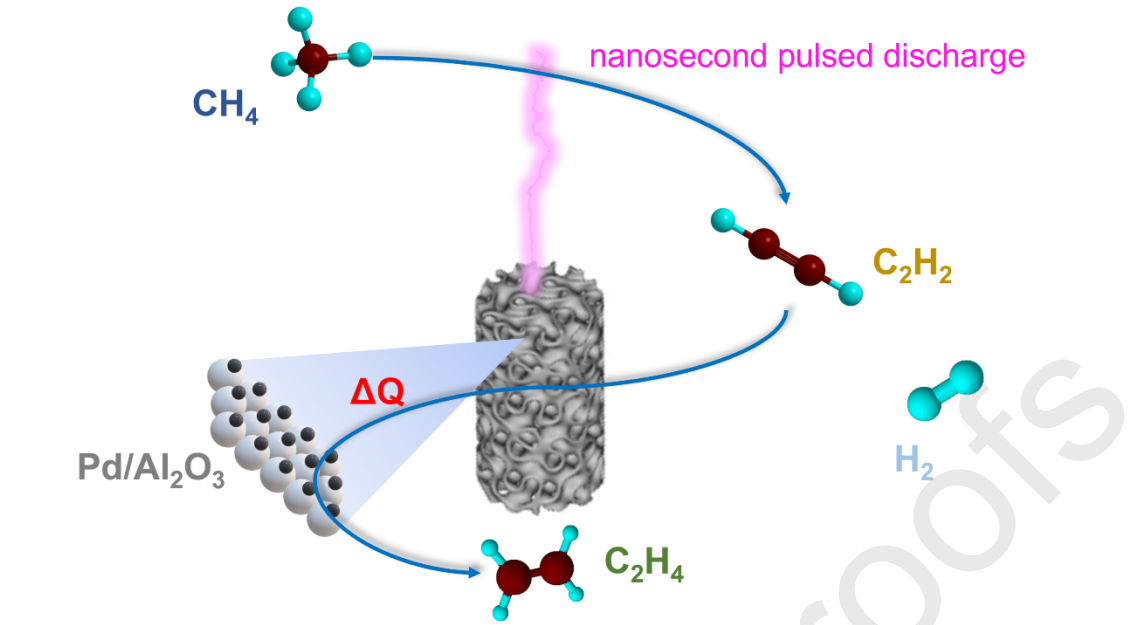

414

415 • Plasma-catalyst thermal integration via additive manufacturing of ground electrode
416 • Totally electrified plasma reactor allows single pass conversion of CH_4 into C_2H_4
417 • 3D-printed structured catalyst intensifies conductive/convective heat transfer
418 • Pd catalyst drives C_2H_2 hydrogenation to C_2H_4 in autothermal fashion
419 • 45% CH_4 conversion and 28% C_2H_4 yield in nanosecond pulsed discharge reactor

420